Applied Physics A (2022) 128:982
https://doi.org/10.1007/s00339-022-06118-3

Applied Physics A
Materials Science & Processing

S.I. : 50TH ANNIVERSARY OF APPLIED PHYSICS

Emerging photonic technologies for cultural heritage studies: the examples of non-linear optical microscopy and photoacoustic imaging

George Filippidis[1] · George J. Tserevelakis[1] · Meropi Mari[1] · Giannis Zacharakis[1] · Costas Fotakis[1,2]

Received: 13 September 2022 / Accepted: 5 October 2022 / Published online: 18 October 2022

Abstract
The availability of non-invasive technologies, which can be used separately or in combination for obtaining chemical composition data and structural information of Cultural Heritage (CH) materials, is of prime importance for improving the understanding the environmental or ageing impact on monuments and artefacts and defining optimal strategies for their conservation. This paper overviews and assesses the potential of two emerging photonic technologies, the Non-linear Optical Microscopy (NLOM) and Photoacoustic (PA) imaging modalities, for a variety of diagnostic applications in preservation science. These techniques, which are well-established in biomedical research, during the last few years have been also investigated as non-invasive tools for the in-depth, high-resolution analysis of various CH objects, including paintings, documents and murals. We discuss on the applicability of these diagnostic optical methods to obtain precise stratigraphic information in artefacts, evaluating additionally the presence and the extent of potential morphological or chemical changes in several CH materials due to ageing. Furthermore, we demonstrate that the contrast complementarity of NLOM and PA imaging provides invaluable insights into the structural integrity of an artwork, which can be subsequently utilized for the early and accurate detection of depth degradation effects.

Keywords Photonic techniques · Non-linear microscopy · Photoacoustic imaging · Diagnosis · Cultural heritage

1 Introduction

Cultural heritage monuments, sites and artefacts are threatened by ageing and a variety of natural and environmental factors such as earthquakes, floods or sea level rise, fires, atmospheric pollution and man-made threats. Therefore, innovative diagnostic technologies for the systematic and accurate monitoring the state of preservation of cultural heritage monuments and artefacts are needed for assessing potential risks and establishing their optimal conversation strategies.

There is a whole range of diagnostic methodologies for the on-site characterization of CH objects. Non-invasive techniques providing chemical information such as Raman and Fourier-Transform InfraRed (FT-IR) spectroscopies [1, 2] have been numerously demonstrated in literature for the in-situ characterization of CH materials of high significance. Furthermore, diagnostic methods such as Optical Coherence Tomography (OCT), Digital Holography and Terahertz imaging [3–5] can reveal structural information and provide a 3D mapping of multi-layered CH media. In addition, other relevant modalities include IR thermography [6], which is used to record the temperature of an object's surface and monitor its variations over time, optical techniques such as Reflected light optical microscopy for superficial observations [7], and elemental analysis methods (e.g., X-Ray Fluorescence Spectrometry [8]) have been extensively used for detailed investigations in CH. On site/remote techniques capable to record the emitted fluorescence or images that reveal the reflectance spectrum of the materials include

George Filippidis and George J. Tserevelakis have contributed equally to this study.

✉ Costas Fotakis
fotakis@iesl.forth.gr

[1] Institute of Electronic Structure and Laser (IESL), Foundation for Research and Technology (FORTH), 71110 Heraklion, Crete, Greece

[2] Physics Department, University of Crete, 71003 Heraklion, Crete, Greece

Laser or LED Induced Fluorescence spectroscopy (LIF) and Multi-spectral Imaging (MSI) [9, 10]. Minimally invasive techniques such as Laser Induced Breakdown Spectroscopy (LIBS) may monitor compositional changes on the surface and in depth and obtain elemental composition [11]. There are also laboratory (ex-situ) techniques that render molecular information for identification and quantification of the crystalline phase composition of the examined CH materials (X-Ray Diffraction) [12]. Moreover, high resolution (nanoscale) morphological, structural and elemental analysis of samples can be acquired via the application of Scanning Electron Microscopy-Energy Dispersive Spectroscopy (SEM–EDS) [13]. It is also feasible to obtain information for the determination of porosity and density of the specimens via porosimetry and helium pycnometry or monitoring thermal stability of the materials through Thermogravimetric analysis (TGA) [14, 15].

All the aforementioned techniques, present advantages and limitations as diagnostic tools in realistic cases since the involved CH materials are numerous and heterogeneous. Thus, there is a need for the development of new techniques to satisfy the variety of diagnostic requirements typically met in several CH studies. In particular, the precise diagnosis of CH artefacts can strongly benefit from the availability of non-invasive methods rendering valuable key information, such as the determination of the different hidden layers composing an artwork, the acquisition of a precise thickness or surface topography, as well as, the identification of the nature of the involved materials and the detection of structural deformities (e.g., delamination or cracks) in the layers. The detailed knowledge of the chemical composition and the in-depth delineation of the physical structure of CH objects with micrometric precision may greatly assist the conservators and art historians to obtain valuable information related to the history of the object, evaluate its authenticity, and provide insights into restorers towards optimized interventions.

Non-linear Optical Microscopy (NLOM) has been widely used to reveal biological structures and functions for accurate diagnosis at cellular and tissue levels [16–18]. The non-linear techniques that commonly employed to image the samples are: Multi-photon excitation fluorescence (MFEF), Second and Third harmonic Generation (SHG, THG). MPEF is a non-linear absorption effect while optical higher harmonic generation procedures including SHG and THG are coherent, non-linear scattering phenomena. SHG and THG are intrinsic properties of the material providing minimal sample disturbance due to their energy conservation characteristics.

NLOM technology has the potential to provide critical information for the fast and reliable in-situ analysis of various CH objects without endangering the integrity of the samples [19]. NLOM techniques are based on the integration of tightly focused near-infrared (NIR) femtosecond laser beams, allowing for the extraction of information from deeper layers of the sample due to the reduced optical scattering of such wavelengths. Moreover, due to the non-linear nature of the process, the NLOM provides high axial and lateral resolution images, intrinsic 3D optical sectioning, and prolonged period of irradiation while minimizing photodamage effects. These significant advantages for CH diagnostics are related to the fact that, in contrast to single-photon techniques, only a small volume of the medium ($\sim 1\mu m^3$) interacts with the laser light, diminishing thermal deposition or other photodamage effects on the object under investigation.

On the other hand, photoacoustic (PA) imaging constitutes one of the most rapidly expanding diagnostic technologies in contemporary biomedical research with diverse applications including the investigation of malignant tumors [20–22], the study of metabolic disorders [23, 24], as well as, the monitoring of drug release processes [25–28]. Within this context, PA methods have been successfully utilized to provide *in-vivo* label-free imaging in a variety of samples ranging from cells and soft tissues to microscopic model organisms and small animals. PA imaging is based on the so-called PA effect, which can be defined as the formation and emission of acoustic waves following the absorption of intensity-modulated (typically pulsed) optical radiation by a material sample. The underlying physical mechanism of the PA effect is thermoelastic; a portion of the absorbed optical energy is converted into heat following non-radiative molecular relaxation, leading to a rapid transient expansion of the absorber and the generation of an initial pressure which typically propagates in the form of broadband ultrasonic waves in the MHz regime. The emitted PA waves can then be detected by employing the same equipment (e.g., piezoelectric elements) as in conventional ultrasound imaging [29].

In the linear regime of PA excitation, the peak-to-peak amplitude of the emitted PA waves is directly proportional to the apparent optical absorption coefficient experienced by the excitation wavelength. As a consequence, PA diagnostic techniques can offer excellent optical absorption contrast features deep inside optically turbid media with high sensitivity and spatiotemporal resolution [30], as the propagating PA waves are attenuated up to three orders of magnitude less compared to NIR optical radiation [31]. Furthermore, the trade-off between imaging depth and spatial resolution can be adjusted according to the acoustic detection bandwidth, as well as, the properties of the optical excitation and acoustic detection elements, permitting thus observations of different specimens at various spatial scales.

In this review article, we present the recent advances in the applications of NLOM techniques with regards to the assessment of the presence and the extent of structural and chemical changes related to the degradation processes affecting the lifespan of several CH materials, such as varnishes,

paintings, lining glues, corrosion layers, historical coatings and parchments. This technology, in the form of three different imaging modalities, provides simultaneously the in-depth compositional characterization of CH objects (via MPEF), the high-resolution morphological delineation (via THG), as well as, the sub-micron distribution of non-centrosymmetric molecules (via SHG), including collagen and starch. Moreover, we give an overview on how PA imaging can break through the barriers of biomedical research to find innovative applications in CH diagnostics. We show that the unique combination of advantages provided by PA signals can be exploited to establish a radically new non-destructive methodology for the uncovering and differentiation of well-hidden features in multi-layered CH objects such as paintings, documents and murals. Furthermore, we demonstrate that the attenuation of the PA waves through optically opaque media (e.g., paints), can be exploited for the precise measurement of the thickness of thin layers. Finally, we present a combined NLOM and PA imaging approach for the high-resolution stratigraphic analysis of multi-layered artworks, providing complementary diagnostic information on the successive layers, including varnish, paints and underdrawings.

2 Overview of the applications of emerging optical diagnostic technologies in CH

2.1 NLOM for CH diagnostics

A characteristic experimental set-up employed for the performance of non-linear imaging measurements in various CH objects is presented in [32]. The values for the lateral and axial resolutions of a non-linear system are ~ 500 nm and ~ 2 μm, respectively.

The first demonstration of NLOM on CH objects involved the sub-micron thickness identification of different natural and synthetic varnish protective layers via THG and their chemical composition discrimination through MPEF measurements [33]. This has been shown both in the transmission and in the reflection modes [34]. Other studies have also demonstrated that MPEF signals can distinguish fresh from aged varnish samples [35]. In addition, SHG and polarization dependent SHG (PSHG) microcopies are able to provide reliable information related to the composition of various types of natural and synthetic adhesives used for conservation or restoration of painted artworks or papers and books of CH and for the quantitative discrimination of aged from fresh starch-based glues, respectively [36, 37]. Another work has appraised the feasibility of NLOM to detect the corrosion layer from silver-based artefacts at high resolution [38]. Moreover, these non-linear imaging techniques have been used to determine the extent of the photochemical damage that could be induced on underlying painting layers during laser removal of varnish protective coatings [39, 40]. This diagnostic approach can lead to the identification of the optimal laser cleaning conditions that induce the minimum collateral damage to the painting layers. MPEF has been applied to the evaluation of phthalocyanine acrylic paint layer thickness [41], to probe the stratigraphy of egg-tempera mock-up paintings [42] and to characterize grisaille paint layers on historical stained glasses [43]. Recently, the same non-linear modality has been employed for the thickness determination of model medieval-like glass layers in a non-destructive manner [44]. Furthermore, non-linear imaging techniques have been applied to extract information from historical coatings samples [45]. Recent works also demonstrated that the degradation procedure in parchments can be revealed by the collection of SHG and PSHG intensity signals [46, 47]. The identification of the safe limits for the use of the non-linear techniques for CH studies has been also investigated. There are works that evaluate the damage of near-infrared femtosecond pulsed lasers and establish safe laser thresholds on a variety of model painted artworks [48]. The target is to determine the exact experimental parameters for the safe irradiation of CH objects. All these applications undoubtably prove that the usage of this optical diagnostic technology can be extremely useful to restoration scientists. It can help CH scientists to reconstruct the history of the sample, evaluate its authenticity, obtain information on the artist technique and provide valuable support to restorers to gain the accurate control of any cleaning interventions.

The main drawback of this technology is the limited penetration depth. The non-linear imaging modalities are preferable to be employed for the extraction of high-resolution information from the outer, transparent in the infrared region, varnish protective layers of artworks. However, despite the severe drop of the non-linear fluorescence signal intensity with increasing depth in paintings, the evaluation of painting stratigraphy with micrometric precision is also feasible, provided a proper interpretation and deconvolution of the non-linear fluorescence response. Figure 1 presents MFEF measurements on a multi-layered sample that simulates a painted artwork. It contains a layer of paint (red lead mixed with linseed oil) and a layer of varnish (dammar dissolved in dichloromethane) on top of it. The MPEF capability to distinguish the different layers of the sample with micrometer resolution is depicted.

The discrimination of the two layers is based on the different fluorescent emission levels detected from the sample. The varnish protective layer presents high transparency in the visible and infrared regions of the spectrum, while it absorbed strongly in the near UV part, thus demonstrating a predominant three-photon excitation mechanism for the employed irradiation wavelength (1030 nm). The underlying paint layer presented strong two and one photon absorption

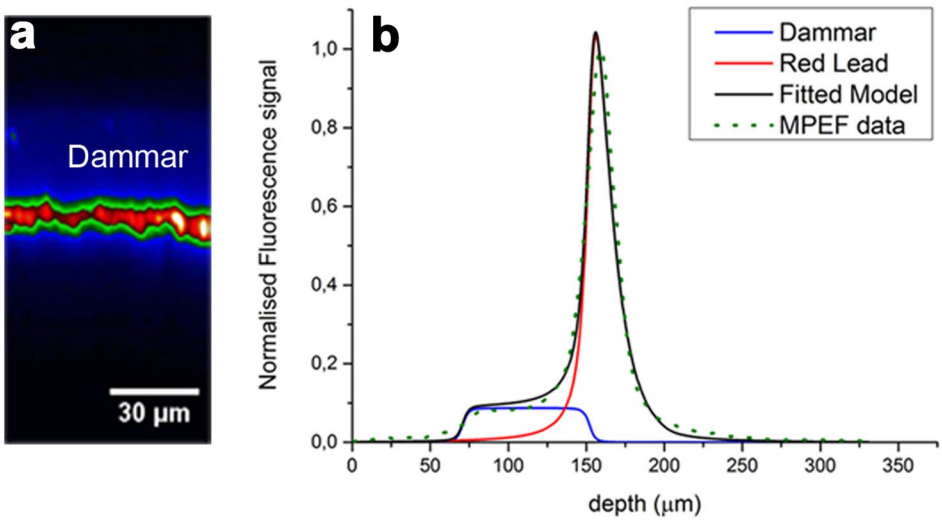

Fig. 1 **a** MPEF cross-sectional imaging of a model multi-layer sample contains a layer of red lead and a layer of dammar. A low intensity fluorescence signal (blue) arises from the layer of dammar, while the painting layer emitted a higher fluorescence (red/green) **b** MPEF signal deconvolution in a z-scan plot profile. The fitted model (black line, $R^2 = 0.99$) was used to decouple the recorded response (green points) into respective signal contributions arising from dammar (blue line) and red lead (red line). The thickness of the dammar varnish measured 82 μm and the thickness of the red led paint layer is 98 μm. Figure adapted from [49]

properties. As it can be observed from Fig. 1, a low intensity MPEF arises from the layer of dammar, while the painting layer emits a higher intensity fluorescence signal. Using a proper simple image processing algorithm, the discrimination and the precise thickness evaluation of the two layers is feasible. The definition of varnish thickness is accomplished due to the transparency of the dammar in the employed infrared excitation wavelength. For the painting layer information about the maximum penetration depth, rather than the thickness of the pigment layer, is obtained due to the high absorption and scattering of the NIR excitation wavelength. The collected data prove that it is possible to acquire in-depth information and discriminate the varnish protective layers from the painting substrate based on the intensity levels of the detected fluorescence signals. Furthermore, the possibility to perform NLOM measurements in the reflection mode enlarges the applicability of this technology to a wide range of real cases.

In painted artworks the most of the frequently used natural varnishes are completely transparent by employing well-established optical techniques such as OCT, and, therefore, impossible to differentiate them. However, the NLOM can provide useful insights for the in-situ characterization of different type of varnishes. Two samples of fresh varnish painted on glass (mastic and dammar) were irradiated at 1030 nm. As depicted in Fig. 2, the detected MPEF intensities are different with mastic more strongly fluorescent than dammar. This difference is due to the different absorption properties of these materials in the near UV part of the spectrum (343 nm) even though both dammar and mastic give three-photon excitation fluorescence. On the other hand, the behavior of aged varnish samples is more complex. Specifically, it has been observed from MPEF imaging that the intensity of fluorescence increases with depth as varnish ages and that NLOM is the appropriate technique for the precise assessment of the degradation of aged natural varnishes as a function of depth [35].

It has to be mentioned that NLOM presents relatively limited depth information. The maximum penetration depth is ~ 500 μm, while it attributes optical diffraction-limited resolution images (hundreds of nanometers in lateral and in the order of one micrometer in axial dimension). Although this approach is not preferable for obtaining information from the deeper layers of CH samples, it can render unique information related to the gradual degradation of artworks [35]. An advantage of this technology is that it provides, by employing a single femtosecond laser beam, complementary information related to the compositional characterization and the sub-micron morphological delineation of CH objects, via the simultaneous detection of different non-linear signals (MPEF, SHG, PSHG, THG).

It has been also demonstrated that NLOM can act synergistically with other well-established optical techniques (OCT, confocal Raman microscopy and terahertz spectroscopy (THz)) rendering additional information for the in-situ fast and reliable analysis of various CH materials [50–52]. OCT offers extended penetration depths in comparison to NLOM. On the other hand, non-linear imaging modalities present improved lateral resolution and similar axial accuracy when compared to OCT. Raman spectroscopy provides

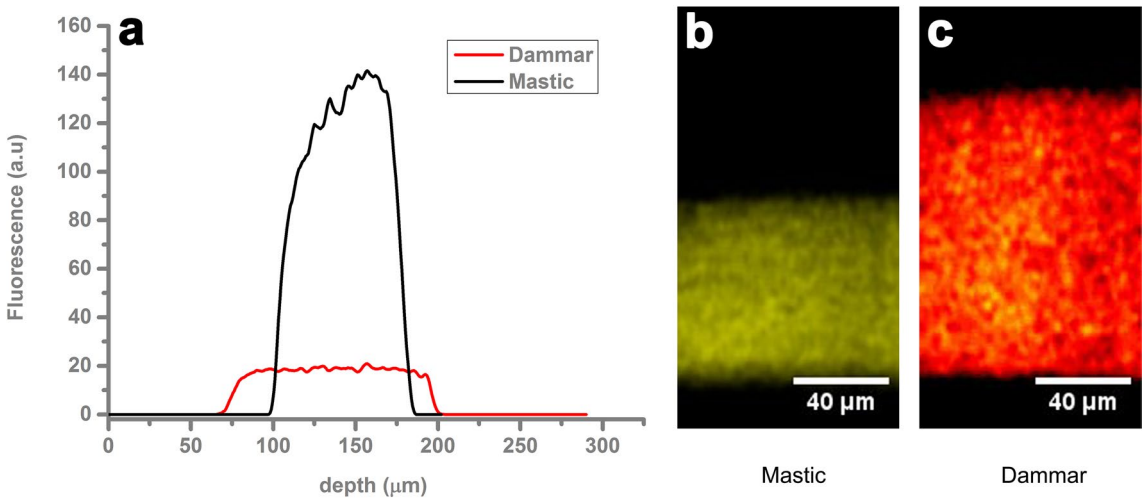

Fig. 2 **a** The thickness of dammar and mastic is measured from MPEF images of **b** fresh mastic and **c** dammar. The level of the detected fluorescence is significantly different between the two materials. Figure adapted from [51]

increased chemical sensitivity and a unique fingerprinting capability of the studied materials but it suffers from the presence of a fluorescence background and it is limited in 2D for highly scattering media. THz imaging reveals underdrawings and information from thick multi-layered samples. However, it is generally an expensive technique with lower spatial resolution compared to NLOM.

2.2 PA imaging methods in CH

The first application of PA imaging in CH diagnostics has been the detection of hidden underdrawings in mock-up painting samples [53]. In this case, the imaging apparatus integrated a Q-Switched Nd:YAG laser source emitting nanosecond pulses at 1064 nm, for the efficient excitation of the signals. The near-infrared (NIR) beam was weakly focused on the reverse side of the mock-up, namely on the canvas support, generating a broad illumination volume as a result of strong scattering. A portion of the scattered photons was strongly absorbed by the graphite sketch regions, inducing the formation of high amplitude broadband PA waves with high specificity. The acoustic signals were subsequently transmitted through the overlying paint layer and the coupling medium (CMC gel) prior their detection by an immersion spherically focused piezoelectric transducer. A maximum amplitude projection (MAP) image was finally formed by raster scanning the mock-up over the beam's focus, revealing the hidden underdrawings with substantially enhanced contrast when compared to the standard NIR imaging in the respective optical spectral region (Fig. 3a–c).

In another study [54], the broad potential of PA imaging has been employed for the diagnostics of layered documents, which constitutes a highly demanding application in terms of spatial resolution, detection sensitivity, imaging contrast and maximum penetration depth. The motivation behind this work is directly related to the fact that the materials that have been used for the generation of documents, (e.g., paper, papyrus or parchment) usually suffer from severe deterioration issues, hindering the access for further investigations without any further risk of damage. Towards this direction, the exploitation of the PA signals generated through the intense absorption of pulsed visible radiation by printed ink, has recovered text characters buried under several layers of stacked paper sheets at high spatial resolution and contrast. Furthermore, the temporal separation of the PA waves arising from the variable distance between the PA sources and the ultrasonic detector, allowed for the discrimination among characters printed on different pages and thus, the layer by layer reading of hidden text (Fig. 3d).

All of the previously presented PA diagnostic technologies have been developed in a transmission geometry, enabling simple and rather straightforward implementations from a technical standpoint. As a consequence, these imaging systems are limited to the investigation of relatively thin objects, not exceeding a couple of millimeters in thickness, hindering the application of the method over a wide range of objects with diverse structural and morphological features. To overcome these restrictions, a novel optimized epi-illumination (reflection-mode) PA imaging system has been built, to provide universal diagnostic information in objects of arbitrary thickness or shape [55]. The capabilities of the epi-illumination PA apparatus were first demonstrated to reveal hidden charcoal, graphite or sinopia sketch drawings in thick concealed (gypsum, limewash, overpainted) wall painting mock-ups [56]. The obtained results provided experimental evidence that the PA signals may provide

Fig. 3 **a** Image of a miniature painting portraying a rural landscape. Scalebar is equal to 1 cm. **b** MAP PA image of the painting's underlying sketch over a central region of $2.2 \times 3.8\,cm^2$, as indicated by the orange box in **a**. **c** Image of the original pencil sketch prior to overpainting. **d** Depth color-coded MAP PA reconstructions of a four-layered mock-up with non-overlapping text in top (XY) and side (XZ, YZ) views. Imaging depth is measured starting from the page facing the illumination side. **e** Image of a thick mock-up covered with a paint layer containing a mixture of titanium white, gypsum and ultramarine blue pigments. Scalebar is equal to 1 cm. **f** MAP PA reconstruction of the hidden graphite underdrawing. Figures adapted from [53–55]

significantly improved imaging contrast when compared to the conventional NIR optical technique in similar spectral regions (Fig. 3e–f).

In an alternative approach, Photoacoustic Signal Attenuation Analysis (PAcSAA) has been recently introduced to provide thickness assessment of optically opaque layers, (e.g., paints) with μm precision [57]. PAcSAA method relies on the generation of strong PA waves by the lower surface of a paint layer, following the absorption of visible radiation. The broadband laser-induced ultrasound is subsequently transmitted through the layer with losses due to the partial conversion of acoustic energy into heat, prior its detection by a spherically focused transducer. The recorded time-domain waveform is analyzed in the Fourier domain to quantify the frequency-dependent attenuation of the PA wave as a function of the layer thickness, using a simple exponential decay model and reference cross-sectional images by an OCT system. The generated calibration curve is then employed for the thickness estimation of an unknown paint layer on a canvas substrate, providing structural information that cannot be easily obtained through pure optical techniques due to strong light scattering. Apart from spot measurements, the PAcSAA method has additionally been demonstrated in the form of an imaging modality combined with underdrawings' mapping [58], by exploiting both the second harmonic (532 nm) and the fundamental (1064 nm) wavelength of a Q-switched Nd:YAG laser source respectively (Fig. 4a–c).

An alternative PA detection method based on the integration of air-coupled ultrasonic transducers has also been shown, in an attempt to avoid the application of coupling media (e.g., water or some compatible gel) in direct contact with the surface of the artwork. Such optimized systems have recently advanced PA technologies towards fully non-contact and non-invasive diagnostic approaches in CH. The promising capabilities of these imaging prototypes have been successfully utilized for the mapping of hidden sketches in painted mock-ups [59], as well as, the detection and study of restoration operations in an oil painting of historical significance [60]. In the latter case, it was observed that the area of the retouching was characterized by weak PA signals, due to the high acoustic attenuation properties of the restoration media, as well as, the back-reflections of

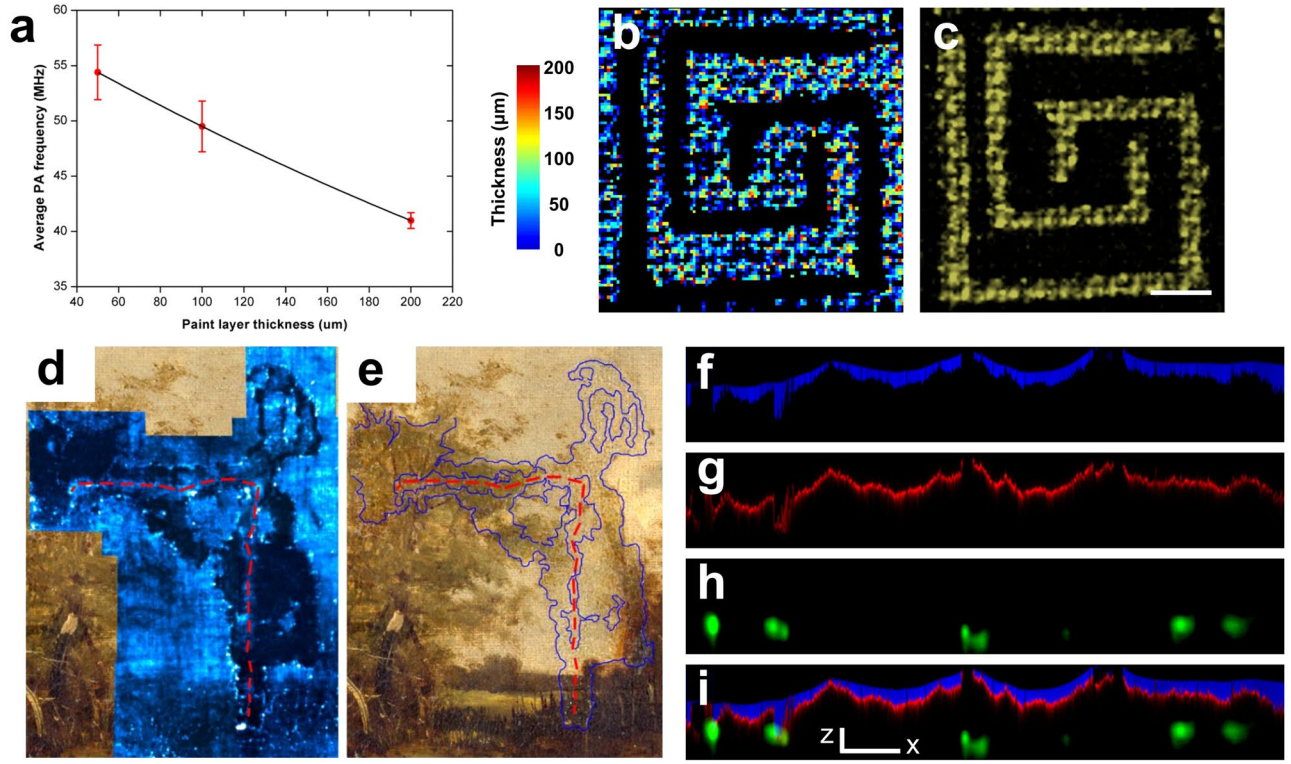

Fig. 4 **a** Plot of the average transmitted PA frequency versus OCT measured thickness for three primary red magenta paint layers. Error bars correspond to the standard deviation of five sequential measurements performed at different regions of the layers. Black line represents the fitting of the experimental points using an exponential decay function, as higher frequencies tend to attenuate more with increased layer thickness. **b** PAcSAA image of color-coded paint thickness values on a painted canvas sample estimated according to the exponentially fitted curve shown in **a**. **c** PA detection of a hidden underdrawing in the same sample using NIR excitation. Scalebar is equal to 2 mm. **d** MAP PA image recorded using a spherically focused air-coupled transducer (cyan hot color map) registered on the RGB image of a historical oil painting. The red-dashed line shows the location of a 7-shaped cut in the painting. **e** RGB image highlighting the outline of the retouching area (blue lines) as revealed by the PA imaging technique. **f** Unmixed cross-sectional MPEF image of the overlying mastic layer in a painted canvas mock-up. **g** Respective MPEF image showing the superficial part of the red lead paint layer. **h** MAP PA image of hidden pencil sketch lines applied directly on the canvas. **i** Composite MPEF and PA image revealing the full stratigraphy of the mock-up sample (Scalebars Z: 100 µm; X: 1 mm). Figures adapted from [57, 58] and [60, 61]

the main signals, resulting from the formation of various acoustic interfaces (Fig. 4d–e).

As has been discussed previously, NLOM approaches have been introduced in the context of CH diagnostics to extend the maximum imaging depth into art media, by exploiting the substantially higher transmissivity of NIR wavelengths. Despite this significant advantage, several materials are optically diffusive to such a degree, that they do not permit observations beyond a few tens of µm in depth using exclusively NIR optical radiation. To address this challenge, a recent work [61] presented an enhanced diagnostic approach in CH by utilizing synergistically both PA and NLOM imaging modalities. By putting emphasis on the stratigraphic analysis of painted artworks, the effective combination of these two techniques could offer complementary diagnostic information together with a high penetration depth in opaque media. Through the application of an optimized deconvolution algorithm, the mixed information carried by a MPEF cross-sectional image of a painted mock-up was decoupled into two contributions arising from the overlying mastic layer (Fig. 4f) and the applied red lead paint (Fig. 4g). On the other hand, the respective PA image of the same region, revealed a hidden pencil sketch on the canvas substrate for the selected plane (Fig. 4h). A composite RGB image merging the different signals, could successfully delineate the full stratigraphy of the investigated sample within the performance limits of the combined modalities (Fig. 4i).

In general, PA imaging provides a lower spatial resolution compared to pure optical microscopy techniques, however, its important advantage lies in the substantially increased imaging depth inside optically diffusive media, arising from the high transmissivity of the generated ultrasonic waves. For the case of acoustic-resolution PA approaches, such as the ones presented previously, the lateral resolution of the recorded images is ultimately restricted by the

diffraction-limited acoustic focus of the transducer, which is typically in the order of a few tens of μm. On the other hand, the maximum imaging depth within the reach of excitation photons is mainly limited by ultrasonic attenuation, thus highly related both to the employed optical wavelength and the frequency content of the PA signals. In this manner, while pure optical microscopy techniques operate in the ballistic photon propagation regime (up to 1 mm in scattering media such as soft tissues), PA diagnostic methods can extend the acquisition of diagnostic information to the optical diffusion regime, reaching otherwise inaccessible imaging depths which exceed 2–3 mm [30]. PA imaging has been directly compared to standard NIR optical imaging with regards to the mapping of hidden underdrawings in CH artefacts [53, 55, 59], demonstrating superior imaging performance in all cases. Furthermore, when compared to other competing diagnostic methods in CH including OCT, X-ray based techniques and THz imaging, PA modalities may offer higher penetration capabilities, improved imaging contrast, as well as, better cost efficiency, respectively [53].

3 Discussion and conclusions

In this paper, we have provided an overview of two emerging photonic technologies for CH studies, namely NLOM and PA imaging. Despite the fact that both of these diagnostic methods were initially applied in the context of biomedical research [62–64], recent implementations have demonstrated their rich potential regarding the detailed investigation of complex multi-layered CH objects including paintings, documents and murals [65].

NLOM imaging offers complementary information on the chemical composition and the physical structure of the studied materials. NLOM modalities, such as MPEF, SHG and THG can be utilized for the stratigraphic analysis and the materials' in-depth profiling in various CH objects. In the last few years, an increased number of research groups worldwide have used non-linear techniques as new diagnostic tools in the service of CH on different artistic materials including varnish, paint, glue, wood, parchment and metal. These studies, reported in this review article, have proven the effectiveness of NLOM in CH science as extremely useful, non-invasive, high resolution, diagnostic tool. They have extracted unique insights that allow for improved restoration operations and optimized cleaning interventions.

Furthermore, the excellent optical absorption contrast provided by PA imaging through the detection of highly transmissive laser-induced ultrasonic waves, has permitted in-depth investigations of optically opaque CH objects, substantially improving the penetration capabilities of pure optical techniques. Nevertheless, to upgrade the application potential of PA technique in CH studies, alternative detection approaches have to be developed [66], eliminating the need for a coupling medium in direct contact with artwork's surface. In this direction, the emergence of high-performance polymer-based piezocomposite ultrasonic detectors in the MHz regime, was shown to provide non-contact PA signal detection in ambient air with high effectiveness [67]. Moreover, optical detection of ultrasound based on refractometric or interferometric methods may provide a different approach for the immersion medium-free recording of broadband PA signals [68, 69]. Another future perspective includes the integration of a multispectral PA excitation scheme through tunable laser sources, enabling the identification of various hidden features exhibiting different optical absorption properties. Apart from the traditional PA excitation wavelengths in NIR and visible, the utilization of mid-IR radiation may additionally provide chemical imaging contrast with several orders of magnitude higher sensitivity compared to Raman signals, as has recently been demonstrated in several biomedical studies [70]. The effective integration of multiple excitation sources ranging from near UV to mid-IR, together with the development of specially designed non-contact PA sensors, will allow for the establishment of a novel, fully non-destructive universal diagnostic methodology in CH, providing complementary stratigraphic information from hidden layers.

The potential of the NLOM and PA modalities for CH diagnostics has been experimentally demonstrated. However, all of the relevant studies have been performed under controlled laboratory conditions. For the broader use in real life CH preservation and definition of conservation strategies, there is need for instrumentation incorporating a hybrid system appropriate for on-site studies. The availability of such a system may offer exceptional capabilities as regards the study and characterization of various types of CH objects at museums and monuments, focusing primarily on the delineation of their historical evolution, state of preservation and overall risk assessment. The challenges of such a transportable, user friendly apparatus will rely on current miniaturization technology, which is already available for biomedical applications.

Acknowledgements The present work was supported by "LASERLAB EUROPE V" (871124).

Author contributions C. Fotakis had the idea for this article. All authors contributed to the study design. The manuscript was written by G. Filippidis and G.J. Tserevelakis. C. Fotakis revised the work. All authors read and approved the final manuscript.

Funding Open access funding provided by HEAL-Link Greece.

Declarations

Conflict of interest The authors declare no competing interests.

Ethics approval Not applicable.

References

1. M.C. Caggiani, P. Colomban, J Raman Spectrosc **42**(4), 790 (2011)
2. M.F. La Russa, S.A. Ruffolo, G. Barone, G.M. Crisci, P. Mazzoleni, A. Pezzino, Int J Spectrosc **2009**, 1–5 (2009)
3. H. Liang, M.G. Cid, R.G. Cucu, G.M. Dobre, A.G. Podoleanu, J. Pedro, D. Saunders, Opt Express **13**(16), 6133 (2005)
4. K. Kosma, M. Andrianakis, K. Hatzigiannakis, V. Tornari (2018) Strain **54**(3).
5. C. Seco-Martorell, V. Lopez-Dominguez, G. Arauz-Garofalo, A. Redo-Sanchez, J. Palacios, J. Tejada, Opt Express **21**(15), 17800 (2013)
6. S. Paoloni, F. Mercuri, N. Orazi, G. Caruso, and U. Zammit, J Appl Phys **128** (18), (2020).
7. F. Ruffinatto, C. Cremonini, N. Macchioni, R. Zanuttini, J Cult Herit **15**(6), 614 (2014)
8. S. Rinaldi, Materiali e Strutture: Problemi di Conservazione **4**, 67 (1994)
9. R. Fantoni, L. Caneve, F. Colao, L. Fiorani, A. Palucci, R. Dell'Erba, V. Fassina, J Cult Herit **14**(3), S59 (2013)
10. R. Hedjam, M. Cheriet, Pattern Recogn **46**(8), 2297 (2013)
11. R. Gaudiuso, M. Dell'Aglio, O. De Pascale, G.S. Senesi, A. De Giacomo, Sensors-Basel **10**(8), 7434 (2010)
12. V. Gonzalez, M. Cotte, F. Vanmeert, W. de Nolf, K. Janssens, Chem-Eur J **26**(8), 1703 (2020)
13. D. Moro, G. Ulian, G. Valdrè, Acta IMEKO **10**, 1 (2021)
14. A.S. Gundogar, C.M. Ross, S. Akin, A.R. Kovscek, J Petrol Sci Eng **146**, 570 (2016)
15. M. Romagnoli, G. Galotta, F. Antonelli, G. Sidoti, M. Humar, D. Krzisnik, K. Cufar, B.D. Petriaggi, J Cult Herit **33**, 30 (2018)
16. N.V. Kuzmin, P. Wesseling, P.C.D. Hamer, D.P. Noske, G.D. Galgano, H.D. Mansvelder, J.C. Baayen, M.L. Groot, Biomed Opt Express **7**(5), 1889 (2016)
17. V. Tsafas, E. Gavgiotaki, M. Tzardi, E. Tsafa, C. Fotakis, I. Athanassakis, G. Filippidis, J Biophotonics **13**(10), (2020).
18. E.E. Hoover, J.A. Squier, Nat Photonics **7**(2), 93 (2013)
19. G. Filippidis, G.J. Tserevelakis, A. Selimis, C. Fotakis, Appl Phys a-Mater **118**(2), 417 (2015)
20. S. Manohar, S.E. Vaartjes, J.C.G. van Hespen, J.M. Klaase, F.M. van den Engh, W. Steenbergen, T.G. van Leeuwen, Opt Express **15**(19), 12277 (2007)
21. S. Mallidi, T. Larson, J. Tam, P.P. Joshi, A. Karpiouk, K. Sokolov, S. Emelianov, Nano Lett **9**(8), 2825 (2009)
22. A. Taruttis, V. Ntziachristos, Nat Photonics **9**(4), 219 (2015)
23. L.H.V. Wang, S. Hu, Science **335**(6075), 1458 (2012)
24. X. D. Wang, X. Y. Xie, G. N. Ku, L. H. V. Wang, J Biomed Opt **11**(2), (2006)
25. S. Kim, Y.S. Chen, G.P. Luke, S.Y. Emelianov, Biomed Opt Express **2**(9), 2540 (2011)
26. H.J. Lee, Y. Liu, J. Zhao, M. Zhou, R.R. Bouchard, T. Mitcham, M. Wallace, R.J. Stafford, C. Li, S. Gupta, M.P. Melancon, J Control Release **172**(1), 152 (2013)
27. L.M. Nie, P. Huang, W.T. Li, X.F. Yan, A. Jin, Z. Wang, Y.X. Tang, S.J. Wang, X.F. Zhang, G. Niu, X.Y. Chen, ACS Nano **8**(12), 12141 (2014)
28. L.M. Nie, X.Y. Chen, Chem Soc Rev **43**(20), 7132 (2014)
29. L.V. Wang, H.-I. Wu, *Biomedical Optics: Principles and Imaging* (Wiley, Hoboken, 2007), pp.283–284
30. J. Yao, L.V. Wang, Photoacoustics **2**(2), 87 (2014)
31. J. Hui, R. Li, E.H. Phillips, C.J. Goergen, M. Sturek, J.X. Cheng, Photoacoustics **4**(1), 11 (2016)
32. M. Mari, V. Tsafas, K. Melessanaki, G. Filippidis, Insight **60**(12), 663 (2018)
33. G. Filippidis, E.J. Gualda, K. Melessanaki, C. Fotakis, Opt Lett **33**(3), 240 (2008)
34. E.J. Gualda, G. Filippidis, K. Melessanaki, C. Fotakis, Appl Spectrosc **63**(3), 280 (2009)
35. G. Filippidis, M. Mari, L. Kelegkouri, A. Philippidis, A. Selimis, K. Melessanaki, M. Sygletou, C. Fotakis, Microsc Microanal **21**(2), 510 (2015)
36. G. Filippidis, K. Melessanaki, C. Fotakis, Anal Bioanal Chem **395**(7), 2161 (2009)
37. S. Psilodimitrakopoulos, E. Gavgiotaki, K. Melessanaki, V. Tsafas, G. Filippidis, Microsc Microanal **22**(5), 1072 (2016)
38. F. Faraldi, G.J. Tserevelakis, G. Filippidis, G.M. Ingo, C. Riccucci, C. Fotakis, Appl Phys a-Mater **111**(1), 177 (2013)
39. P. Vounisiou, A. Selimis, G.J. Tserevelakis, K. Melessanaki, P. Pouli, G. Filippidis, C. Beltsios, S. Georgiou, C. Fotakis, Appl Phys a-Mater **100**(3), 647 (2010)
40. M. Oujja, S. Psilodimitrakopoulos, E. Carrasco, M. Sanz, A. Philippidis, A. Selimis, P. Pouli, G. Filippidis, M. Castillejo, Phys Chem Chem Phys **19**(34), 22836 (2017)
41. A. Dal Fovo, M. Oujja, M. Sanz, A. Martinez-Hernandez, M.V. Canamares, M. Castillejo, R. Fontana, Spectrochim Acta A **208**, 262 (2019)
42. A. Dal Fovo, M. Sanz, M. Oujja, R. Fontana, S. Mattana, R. Cicchi, P. Targowski, A. Sylwestrzak, A. Romani, C. Grazia, G. Filippidis, S. Psilodimitrakopoulos, A. Lemonis, M. Castillejo, Sustainability-Basel **12**(9), (2020)
43. M. Oujja, F. Agua, M. Sanz, D. Morales-Martin, M. Garcia-Heras, M. A. Villegas, M. Castillejo, Talanta **230**, (2021)
44. M. Oujja, T. Palomar, M. Martinez-Weinbaum, S. Martinez-Ramirez, M. Castillejo, Eur Phys J Plus **136**(8), (2021)
45. G. Latour, J.P. Echard, M. Didier, M.C. Schanne-Klein, Opt Express **20**(22), 24623 (2012)
46. G. Latour, L. Robinet, A. Dazzi, F. Portier, A. Deniset-Besseau, M. C. Schanne-Klein, Sci Rep-Uk **6**, (2016)
47. M. Schmeltz, L. Robinet, S. Heu-Thao, J. M. Sintes, C. Teulon, G. Ducourthial, P. Mahou, M. C. Schanne-Klein, G. Latour, Sci Adv **7**(29), (2021)
48. A. Dal Fovo, M. Sanz, S. Mattana, M. Oujja, M. Marchetti, F. S. Pavone, R. Cicchi, R. Fontana, M. Castillejo, Microchem J **154**, (2020)
49. M. Mari, G. Filippidis, Sustainability-Basel **12**(4), (2020)
50. A. Nevin, D. Comelli, I. Osticioli, G. Filippidis, K. Melessanaki, G. Valentini, R. Cubeddu, C. Fotakis, Appl Phys a-Mater **100**(3), 599 (2010)
51. H. Liang, M. Mari, C.S. Cheung, S. Kogou, P. Johnson, G. Filippidis, Opt Express **25**(16), 19640 (2017)
52. G. Filippidis, M. Massaouti, A. Selimis, E.J. Gualda, J.M. Manceau, S. Tzortzakis, Appl Phys a-Mater **106**(2), 257 (2012)

53. G. J. Tserevelakis, I. Vrouvaki, P. Siozos, K. Melessanaki, K. Hatzigiannakis, C. Fotakis, G. Zacharakis, Sci Rep-Uk **7**, (2017)
54. G. J. Tserevelakis, M. Tsagkaraki, P. Siozos, G. Zacharakis, Strain **55**(2), (2019)
55. G. J. Tserevelakis, A. Chaban, E. Klironomou, K. Melessanaki, J. Striova, G. Zacharakis, J Imaging **7**(9), (2021)
56. A. Chaban, G. J. Tserevelakis, E. Klironomou, R. Fontana, G. Zacharakis, J. Striova, J Imaging **7**(12), (2021)
57. G. J. Tserevelakis, A. Dal Fovo, K. Melessanaki, R. Fontana, G. Zacharakis, J Appl Phys **123**(12), (2018)
58. A.D. Fovo, G.J. Tserevelakis, A. Papanikolaou, G. Zacharakis, R. Fontana, Opt Lett **44**(4), 919 (2019)
59. G.J. Tserevelakis, P. Siozos, A. Papanikolaou, K. Melessanaki, G. Zacharakis, Ultrasonics **98**, 94 (2019)
60. A. Dal Fovo, G. J. Tserevelakis, E. Klironomou, G. Zacharakis, R. Fontana, Eur Phys J Plus **136**(7), (2021)
61. G.J. Tserevelakis, V. Tsafas, K. Melessanaki, G. Zacharakis, G. Filippidis, Opt Lett **44**(5), 1154 (2019)
62. G.J. Tserevelakis, S. Psycharakis, B. Resan, F. Brunner, E. Gavgiotaki, K. Weingarten, G. Filippidis, J Biophotonics **5**(2), 200 (2012)
63. G.J. Tserevelakis, K.G. Mavrakis, D. Pantazopoulou, E. Lagoudaki, E. Detorakis, G. Zacharakis, Opt Lett **45**(20), 5748 (2020)
64. G. J. Tserevelakis, S. Avtzi, M. K. Tsilimbaris, G. Zacharakis, J Biomed Opt **22**(6), (2017)
65. G. J. Tserevelakis, P. Pouli, G. Zacharakis, Herit Sci **5**(1), (2020)
66. Z. Hosseinaee, M. Le, K. Bell, P. H. Reza, Photoacoustics **20**, (2020)
67. X. L. Dean-Ben, G. A. Pang, F. M. de Espinosa, D. Razansky, Appl Phys Lett **107**(5), (2015)
68. B.Q. Dong, C. Sun, H.F. Zhang, Ieee T Bio-Med Eng **64**(1), 4 (2017)
69. G. Wissmeyer, M. A. Pleitez, A. Rosenthal, V. Ntziachristos, Light-Sci Appl 7(2018).
70. M.A. Pleitez, A.A. Khan, A. Solda, A. Chmyrov, J. Reber, F. Gasparin, M.R. Seeger, B. Schatz, S. Herzig, M. Scheideler, V. Ntziachristos, Nat Biotechnol **38**(3), 293 (2020)